



Lower Miocene Glacimarine Gravity Flows, Cape Roberts Drillhole-1, Ross Sea, Antarctica

J.A. HOWE^{1,*}, K.J. WOOLFE² & C.R. FIELDING³

¹British Antarctic Survey, High Cross, Madingley Road, Cambridge, CB3 0ET - UK

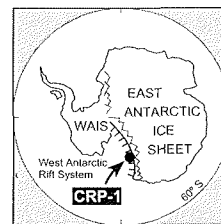
*Present Address: Scottish Association for Marine Science, Dunstaffnage Marine Laboratory, PO Box 3,
Oban, Argyll, PA34 4AD - UK

²Department of Geology, James Cook University, Townsville, Q 4811 - Australia

³Department of Earth Sciences, University of Queensland, Queensland 4072 - Australia

Received 15 July 1998; accepted in revised form 25 October 1998

Abstract - Nineteen samples of the Cape Roberts-1 drillcore were taken from Miocene deposits, from 90.25 - 146.50 metres below seafloor (mbsf) for thin section and laser grain-size analysis. Using the grain-size distribution, detailed core logging, X-radiography and thin-section analysis of microstructures, coupled with a statistical grouping of the grain-size data, three main styles of gravity-flow sedimentation were revealed. Thin (centimetre-scale) muddy debris-flow deposits are the most common and are possibly triggered by debris rain-out from sea-ice. These deposits are characterised by very poorly sorted, faintly laminated muddy sandstones with coarse granules toward their base. Contacts are gradational to sharp. Variations on this style of mass-wasting deposit are rhythmically stacked sequences of pebbly-coarse sandstones representing successive thin debris-flow events. These suggest very high sedimentation rates on an unstable slope in a shallow-water proximal glacimarine environment. Sandy-silty turbidites appear more common in the lower sections of the core, below approximately 141.00 mbsf, although they occur occasionally with the debris flow deposits. The turbidites are characterised by inversely to normally graded, well-laminated siltstones with occasional limestones, and represent a more distal shallow-water glacimarine environment.



INTRODUCTION

The main questions to be addressed by the Cape Roberts Project are: what is the history and extent of the East Antarctic Ice sheet, and what was the rifting history of the Ross Sea and the Transantarctic Mountains? To answer these questions, the full range of depositional processes needs to be evaluated. Previous drilling projects in this region have sampled Eocene-Early Oligocene rocks (MSSTS-1 and CIROS-1), and whilst the drillcore displayed some sedimentary evidence for nearby grounded ice and some limited sea ice distribution, evidence of the onset of glaciation was not recovered (Barrett, 1996; Fielding et al., 1997). Other work on the sedimentology and palaeo-environment of the CRP-1 core include Fielding et al. (this volume) and Powell et al. (this volume). These authors describe the Lower Miocene section of the core as being deposited in a shallow marine environment with a polythermal glacier, grounded in tidewater with occasional icebergs rafting coarser debris beyond the terminus. This environment would have produced very rapid sedimentation of grounding-line fans, morainal banks and ice-rafted debris (Cape Roberts Science Team, 1998). This study attempts to identify and classify the variety of gravity flows occurring in this dynamic, shallow-water environment using a statistical analysis of grain size data, thin sections and detailed core logs.

REGIONAL SETTING

The Cape Roberts-1 (CRP-1) drillsite was located on sea-ice 15 km east of Cape Roberts, during October 1997. CRP-1 is the most offshore of a planned series of three drillsites, scheduled for drilling in the seasons of the austral spring 1998 and 1999. McMurdo Sound lies at the southwestern end of the Ross Sea, between the Transantarctic Mountains and the Pliocene-age volcanic Ross Island. The Cape Roberts drillsite lies on the offshore bathymetric rise, of Roberts Ridge, rising from 500 m water depth to less than 100 m. Erosion by glacial advances has truncated Roberts Ridge and exposed the eastward dipping strata of the Victoria Land Basin. CRP-1 drilled to a depth of 147.69 m in water depths of 150 m. The recovered drillcore has been provisionally dated by *in situ* diatom biostratigraphy as being Quaternary age (1.25-1.80 Ma), above an unconformity at 43.15 mbsf (revised boundary: Fielding et al., this volume) and lower Miocene age (17.5-22.4 Ma) between 43.55-147.69 mbsf (Cape Roberts Science Team, 1998).

METHODS

Following detailed logging, X-ray images of the half-core sections were obtained using a Torrex 120-D

X-radiographic machine, in the Crary Laboratory, McMurdo Station. This system operated using real-time video imagery recorded as the 1 m sections were passed through the system. The images were recorded on S-VHF (NTSC system) video tapes before any sampling had taken place. Exposure settings were around 4 mA and 85 kV. Nineteen thin sections have been collected from lithostratigraphic Units 5.7 to 7.1 (90.25 to 146.50 mbsf), and include sandstones, diamicts and claystones (Tab. 1). Thin sectioning of the sediments proved difficult because they are friable. Of the nineteen samples, only nine could be oriented and remained intact. The sediments were vacuum impregnated using Araldite AY105 resin and Araldite HT972 hardener, and cured overnight at 55°C. The resulting blocks were planed flat using fixed or loose abrasive, or both. Some were planed dry, and some used Ethanediol as a lapping fluid. Normal thin-sectioning techniques were then used, using a Logitech LP30 to produce finished thin sections. The Malvern laser sizer analysed the samples for particle-size distributions and resulting data were grouped using a statistical software package called Entropy. Samples were soaked in tap water for 24 hrs and then treated with 10% HNO₃ to remove carbonate. They were then disaggregated in an ultrasonic bath until microscopic inspection confirmed disaggregation was complete. The samples were then washed and sieved at 2 000 microns to remove the gravel fraction, dried at 60°C, and finally mixed with water to form a thick paste. Subsamples were resuspended in water and ultrasonically dispersed for 15 seconds prior to grain-size determination. Grain-size determinations were made in 32 size classes using 15 000 laser-diffraction observations collected on a Malvern Mastersizer-X. The data were exported into a spreadsheet using a modification of Woolfe & Michibayashi's (1995) DDE link and sample grouping was achieved using a much improved version of Woolfe & Michibayashi's (1995) Entropy program.

LITHOLOGIES

THIN-SECTION ANALYSIS

Of the nineteen thin-section samples taken (see Tab. 1), nine were oriented samples. Units 5.7 - 7.1 were sampled including sediment types from fining-upward sandstone to laminated claystones (Fig. 1).

THIN-SECTION / LITHOSTRATIGRAPHIC UNIT DESCRIPTION

Unit 5.7 contains fine-to-massive sandstone and fining-upwards sandstone. Sub-rounded to rounded quartz grains are dominant, with a low percentage of interstitial clays. The unit is very poorly sorted comprising 80% quartz grains. Feldspars, lithic grains and opaque minerals occur. Also present are possible igneous, euhedral phaneritic crystals, and clasts of crystalline volcanic and intrusive rocks.

Unit 5.8 is a weakly-bedded to well-laminated sandstone. Faint laminae of quartz-rich sediments are visible, with subangular to subrounded shape, and the

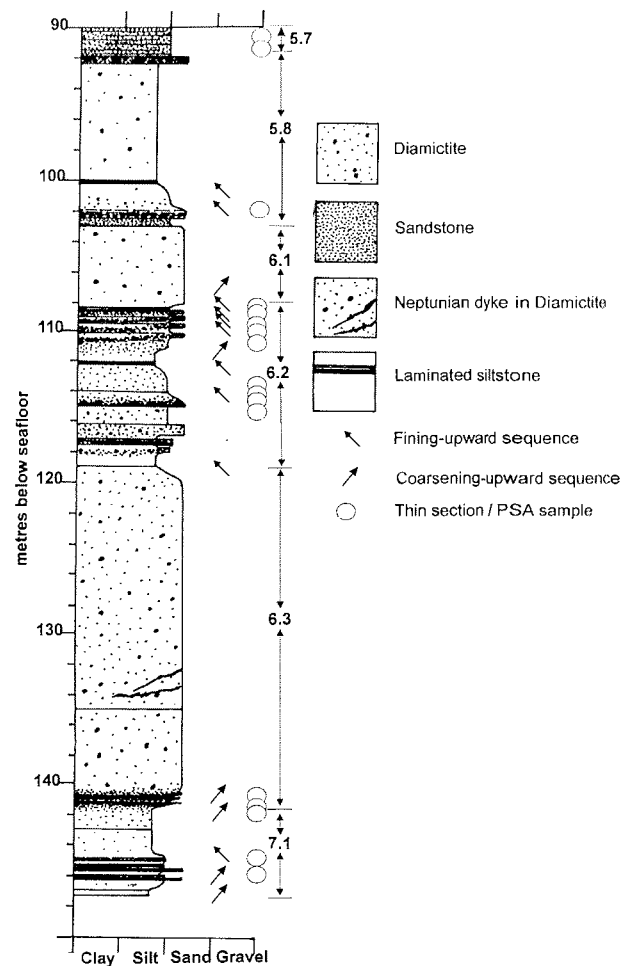


Fig. 1 - Summary lithological log for the lower Miocene sequence of the CRP-1 core. Sample intervals are shown by open circles and coarsening and fining sequences are indicated by arrows. Also shown are the lithostratigraphic units.

sediment is very poorly sorted. Some varieties of igneous material are common.

Unit 6.2 comprises stratified, fining upwards-to-reverse graded and more massive sandstones. The sediment is dominated by subangular to subrounded, quartz with common feldspars, amphiboles, pyroxenes and some variable interstitial clay component. The sediment is very poorly sorted. Also present are possible common fragments of Gallipoli Volcanic Group (Devonian) rhyolites in Sample 108.94-108.95 (with reverse grading) and 109.65-109.66. Igneous crystalline growth textures are common with plagioclase twinning and microcline present. Some rare, faint, laminae of the quartz grains are visible.

Unit 6.3 is a clayey, faintly laminated, siltstone. The sediment is poorly sorted with subangular to subrounded, silt-sized quartz grains dominant. Small millimetre-scale lamination is present in the core surface. Some sharp contacts between the silts and the clays are common.

Unit 7.1 is dominated by a well-laminated siltstone and more massive claystone. These are massive towards the base becoming increasingly laminated towards the top of the samples. Sharp contacts are common between the silt and clays. A high percentage of interstitial clays, between the subangular quartz grains is common. The

Tab. 1 - Summary of sample information, and classification of gravity-flow type.

Sample Interval	Lithology (Unit)	Comment	Interpretation
90.25-90.27	Unit 5.7 Fining upwards sdst	loose	background
91.99-92.00	Unit 5.7 Fine sdst	loose	background
102.89-102.90	Unit 5.8 Weakly bedded well laminated sdst	loose	debrite
108.86-108.87	Unit 6.2 Stratified sdst	loose	turbidite
108.94-108.95	Unit 6.2 Stratified sdst	Oriented	turbidite
109.25-109.26	Unit 6.2 Fining upward sdst	loose	debrite
109.31-109.32	Unit 6.2 Fining upward sdst	loose	debrite
109.45-109.46	Unit 6.2 Fining upwards sdst	Oriented	debrite
109.65-109.66	Unit 6.2 Fining upwards sdst	Oriented	background
114.10-114.11	Unit 6.2 Massive silty-coarse sdst	loose	background
114.38-114.39	Unit 6.2 Massive silty-coarse sdst	loose	debrite
114.86-114.87	Unit 6.2 Fining upward sdst	loose	debrite
115.03-115.04	Unit 6.2 Fining upward sdst	loose	debrite
141.43-141.46	Unit 6.3 Clayey siltstone	Oriented	turbidite
141.45-141.46	Unit 6.3 Clayey siltstone	Oriented	turbidite
141.50-141.51	Unit 6.3 Clayey siltstone	Oriented	turbidite
144.82-144.83	Unit 7.1 Laminated siltstone	Oriented	turbidite
145.82-145.83	Unit 7.1 Massive claystone	Oriented	turbidite
146.49-146.50	Unit 7.1 Massive claystone	Oriented	turbidite

laminae are irregular with bifurcation common. The more massive silty clays contain no laminae.

X-RADIOGRAPHS

The X-radiography performed at the Cray laboratory provides some valuable insights into the internal structure of some intervals of the core. In particular, the normally graded sandy lamination (*e.g.* 145.80 mbsf) is visible in the thinly laminated units and the coarse, poorly sorted diamicts (*e.g.* 109.25 mbsf) also display some internal structure, such as reverse or normal grading not always noted in the visible core surface.

PARTICLE SIZE ANALYSIS / ENTROPY GROUPING

Grain-size distribution curves were produced for each of the nineteen samples analysed. Grain size analysis can be used to infer some depositional processes, with, in some cases, the degree of sorting indicative to the depositional environment. A simple example of this are the grain-size differences between turbidites and debris flows. Studies from the Nova Scotian slope (Stow, 1979) and the Hebrides slope (Howe, 1995) have shown that the more well-sorted the sediment, the greater the degree of transport. For turbidity- and debris-flow events, the differences are clear with the turbidity currents potentially depositing the more well-sorted sediment compared to the slower moving, admixtures of debris flows. The problem becomes somewhat simplified in a glacial environment, where the original source sediment can be very poorly sorted; thus any sorting trends can, to a certain extent, be assumed to be the result of transportation. Further high latitude studies have demonstrated how effective this technique can be at determining the depositional process of a sediment, when combined with other sedimentological techniques such as detailed logging and X-radiography (Wright & Anderson, 1982; Hein et al., 1990; Akhurst, 1991).

Entropy grouping is a statistical technique for grouping sediments with like particle-size characteristics. On the basis of the particle-size analysis combined with the statistical Entropy grouping, five main subdivisions of the data were realised. Grain-size distributions varied from moderately well sorted sands with a mode in the fine-medium range (150-300 μm) to very poorly sorted sediments with multi-modal distributions from clays (4 μm) to very coarse sands (1 000 μm). Grain size plots are shown in figure 2.

ENTROPY ANALYSIS

Entropy is a statistical technique which measures the degree of variation within a table of data. Each sample in the table or matrix describes the distribution of one or many variables at a particular point in time or space. The total inequality, or regularity statistic, $I(Y)$ for all the samples in the data matrix is calculated as:

$$I(Y) = \sum_{j=1}^J Y_j \sum_{i=1}^N Y_{ij} \log_2 2NY_i$$

where: Y_j = frequency value in class j ; J = number of analysed elements; N = number of samples (rows); Y_i = frequency value in class j that are sample i , such that $Y_i = Y_{ij}/Y_j$; Y_{ij} = proportion of the total population (all of N samples) in row i , column j . Then

$$\sum_{j=1}^J Y_j = 1.0 \quad \text{and} \quad \sum_{i=1}^N Y_i = 1.0$$

For a data matrix of grain size measurements, J is the number of grain size classes analysed. The $I(Y)$ statistic is a measure of the inequality in the distribution of class values over all the samples, weighted by the amount of each grain size in the sample.

When the data matrix is divided into two or more groups, the inequality statistic $I(Y)$ may be decomposed into a within- and between-group inequality which, when summed, give the value of $I(Y)$. Since the between- and within-group inequalities are interdependent, only one of these measurements is required to classify a grouping. The

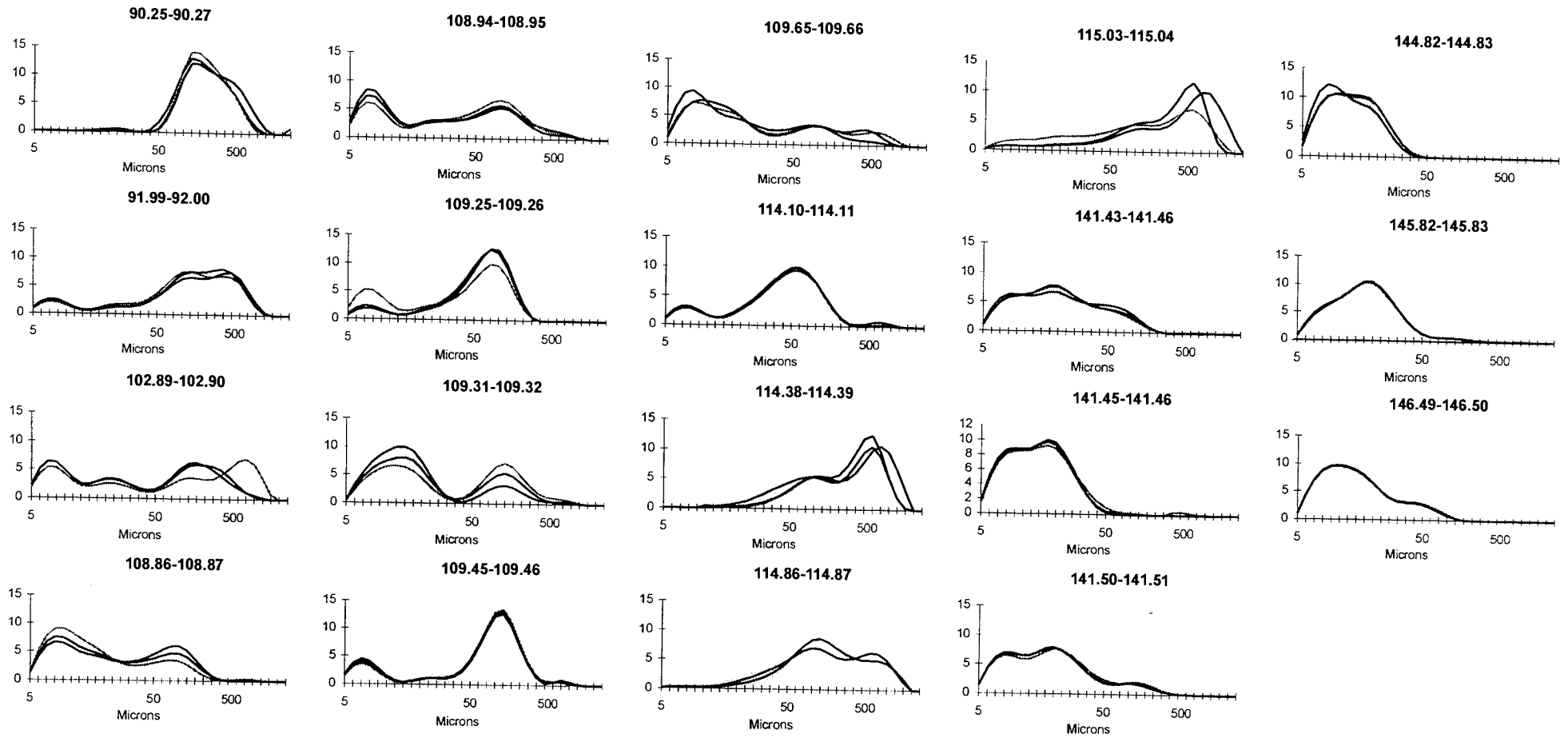


Fig. 2 - Summary grain-size plots for the nineteen samples. Each sample was analysed three times. The shaded box represents coarse silt-sized sediment.

between-group inequality is used for convenience and is calculated using the formula:

$$IB(Y) = \frac{\sum_{j=1}^J Y_j \sum_{r=1}^R Y_{jr} \log 2^{\frac{Y_{jr}}{N \cdot X}}}{N \cdot X}$$

where R = total number of groups (r) and $I_B(Y)$ = between group inequality.

The maximum value of IB is $I(Y)$, when all the samples within each group are exactly the same. The minimum value is 0, when all the samples in the data matrix are the same.

For a data matrix of N samples, there is a finite number of ways they can be divided into G groups, where G is between 1 and N. The aim of the exercise is to find the optimum grouping of the nineteen grain-size samples when G is fixed. Therefore, it is necessary to calculate a parameter which allows grouping solutions to be compared. This is achieved by taking the between-group inequality and dividing by the total inequality to produce a value called Rs, which is usually presented as a percentage. The Rs value quantifies to what degree the inequality in the whole dataset is explained by a particular grouping solution. Larger values of Rs indicate statistically better groupings. For increasing numbers of groups, the Rs statistic will also increase. For one group, the between-group inequality is zero and so is the Rs value; for N groups, $I_B(Y)$ is equal to $I(Y)$ and Rs is 100 because all the data's inequality can be explained by having each sample in its own group. For a data matrix consisting of well-grouped data, a graph of Rs against the number of groups will produce a convex curve, and for a purely random distribution the line will be straight. In the first instance, the optimum number of groups for that dataset will be the point at which increasing the number of groups produces a smaller change in the Rs value, *i.e.* the inflection point of the curve.

In order to classify a data matrix into groups, the value of $I(Y)$ is calculated for the matrix and that of $I_B(Y)$ is calculated for each grouping. With large datasets of tens or hundreds of samples and about 30 size classes in each sample, it is necessary to use a computer program to find the optimum classification. Johnston & Semple (1983) included a FORTRAN program listing for this procedure in their monograph. Woolfe & Michibayashi (1995)

produced a QUICKBASIC translation of the program called ENTROPY 4.2.

RESULTS

Plotting the number of groups against the Rs statistic is a generally accepted method of determining optimum entropy groups (Semple et al., 1972). In this example 3, 4 or 5 groups may be considered as potentially optimal. We have chosen to use five entropy groups because this number is close to the statistical optimum and gives the best textural resolution. The results of this clustering using all of the sample replicates are presented in table 2.

In this clustering, repeat runs of samples 102.89-102.90 and 108.86-108.87 lead to an outlier being grouped separately from the other two results. In both cases the outlier is sample A (*i.e.* the first of the repeats to be run). In the case of the sample at 102.89-102.90, the discrepancy is caused by a coarse-grained 600-750 μm peak and this almost certainly represents residual contamination from a previous sample. However, the sample 108.86-108.87 discrepancy represents a slight increase in finer-grained material in the first run sample. However, inspection of the size-frequency distribution reveals that the difference is very small suggesting that a five group solution of this dataset is close to the limit of experimental error.

CLASSIFICATION OF DOWNSLOPE MOVEMENTS

Based upon the lithological evidence, X-radiographs and the grain-size analysis, and supported by the five statistical groupings of the grain-size data, the nineteen samples can be grouped into three with a further smaller subgroup (Tab. 1, Fig. 3). The interpretations of the three main lithofacies groups are as follows :

- 1) Normal glacimarine, background sediments. These are characterised by homogeneous massive sands or silts with limestones and pervasive intense bioturbation throughout. These sediments may be result of slow, low energy deposition with material falling out of

Tab. 2 - Entropy grouping analysis.

Group 1	Group 2	Group 3	Group 4	Group 5
114.38-114.39A	141.43-141.46A, B & C	90.25-90.27A	102.89-102.90B	114.10-114.11A
114.38-114.39B	141.43-141.46B	90.25-90.27B	102.89-102.90C	114.10-114.11B
114.38-114.39C	141.43-141.46C	90.25-90.27C	108.86-108.87B	114.10-114.11C
114.86-114.87A	141.45-141.46A		108.86-108.87C	109.25-109.26A
114.86-114.87B	141.45-141.46B		108.94-108.95A	109.25-109.26B
115.03-115.04A	141.45-141.46C		108.94-108.95B	109.25-109.26C
115.03-115.04B	141.50-141.51A		108.94-108.95C	109.45-109.46A
115.03-115.04C	141.50-141.51B		109.31-109.32A	109.45-109.46B
91.99-92.00A	141.50-141.51C		109.31-109.32B	109.45-109.46C
91.99-92.00B	144.82-144.83A		109.31-109.32C	
91.99-92.00C	144.82-144.83B		109.65-109.66A	
102.89-102.90A	144.82-144.83C		109.65-109.66B	
	145.82-145.83A		109.65-109.66C	
	145.82-145.83B			
	145.82-145.83C			
	146.49-146.50A			
	146.49-146.50B			
	146.49-146.50C			
	108.86-108.87A			

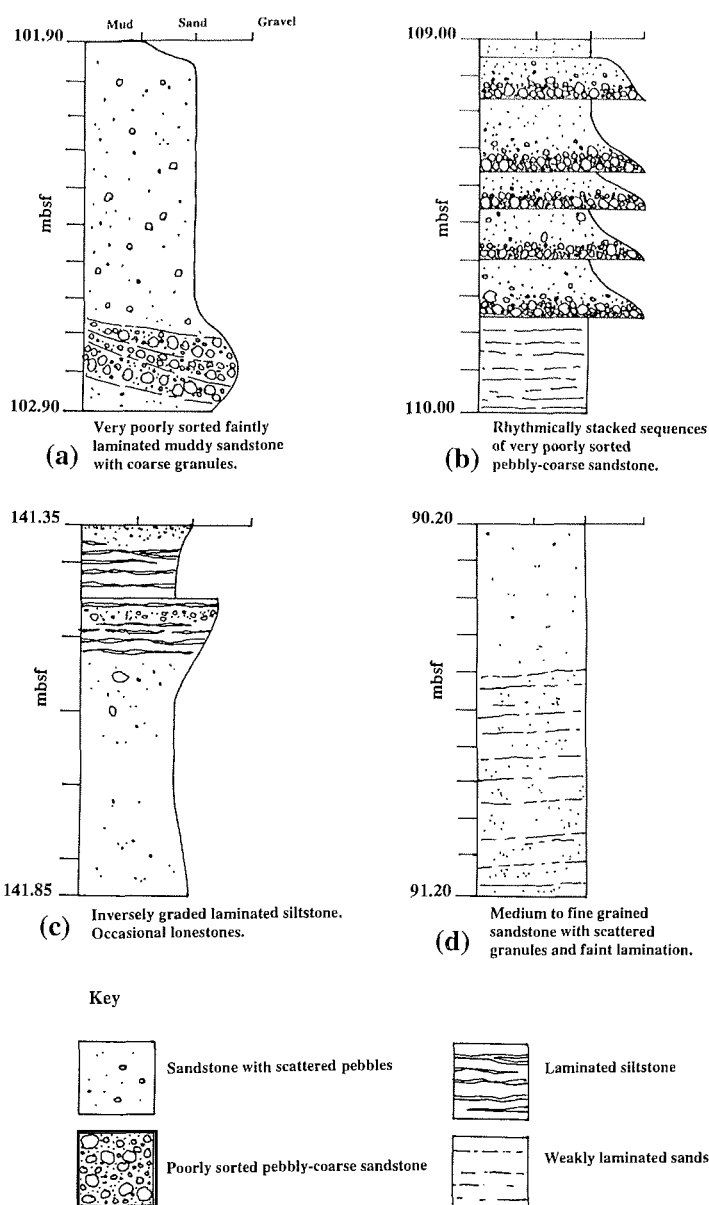


Fig. 3 - Lithological plots showing the CRP-1 drillcore with graphic examples for each of the main gravity-flow types described in the text.

suspension and becoming mixed by a diverse infauna. This material is similar to the finer-grained more distal glacimarine deposits reviewed by Eyles et al. (1985).

- 2) Muddy small-scale (cms)-scale debris-flow deposits are very poorly sorted and normally or inversely graded with sharp or gradational contacts. They have little or no bioturbation (possibly due to the nature of the sediment) and some lamination is preserved (Pickering et al., 1989). Lags of coarser grains are preserved. These small-scale, thin debris-flow deposits may possibly be triggered by ice-rafting onto rapidly sedimenting glacimarine slopes in shallow water. A further subgroup of these is developed in 108-109 mbsf where a rhythmic, stacked sequence of thin debris-flow deposits occur.
- 3) High-density turbidites characterised by well-laminated sands and silts are common (Hill, 1984; Eyles et al., 1985; Pickering et al., 1989). Laminae are preserved

within normally or inversely graded coarsening and fining cycles. Laminae are more massive at the base, becoming graded towards finer, bioturbated material at the top. Some coarser lags are developed within the sand laminae. Bioturbation is absent in these horizons and sharp contacts with the surrounding sediments are sharp. This type of sedimentation is more common below 141.43 mbsf to the end of the core.

DISCUSSION

Wherever they occur, gravity-flow deposits are an indicator of high sedimentation rates, with sediments being deposited rapidly onto an unstable slope in any depth of water. Glacimarine gravity-flow events have been discussed by a number of authors from a variety of slope settings, from deep-water, typically large events (e.g. The Bear Island Fan; Dowdeswell et al., 1997) to the

thin, intermediate water mid-latitude debris flows (Hebrides Slope, North Atlantic; Howe, 1995). In the shallow-water setting (less than 200m) of the Miocene of CRP-1 drillcore, the environment is thought to be one of a polythermal glacier extending seaward from the lower Transantarctic Mountains, occasionally covering the drillsite (Cape Roberts Science Team, 1998; Powell et al., this volume). Gravity flows of this type in Ross Sea drillcores have been described from the CIROS-1 and 2, DVDP-11, MSSTS cores as well the CRP-1 core (Barrett et al., 1987; Barrett & Hambrey, 1992; Fielding et al., 1997). Modern analogues for thin debris-flows can be made with sedimentation along an ice front in Alaska (Eyles et al., 1985). Bartek & Anderson (1991) discussed turbidites, grain-flow deposits and debris-flow deposits from piston cores from eastern McMurdo Sound as being the commonest style of deposition during interglacials. The style of gravity flows may also be loosely associated with the location of a proximal glacial terminus with the deposition of muddy debris-flows and stacked sequences of debris flows. The turbidites maybe deposited more distal to the glacial terminus. The gravity-flow events represented in CRP-1 are most likely to be the direct result of rapid sedimentation in a shallow water glacimarine environment. Unstable glacimarine fans or deltas as described by Powell et al. (this volume) are possible sources of the flows. Sediments are fed into the fans from the terminus and the rapid sedimentation produces poorly sorted sediments on an unstable slope. Triggering sources remain unknown, although either an oversteepening of the slope, or iceberg grounding is likely. With an increasing distance from the source (or a retreat of the ice), the debris flows become high-density turbidity currents and more distal muddy turbidity currents. The environment may also have been relatively quiet water, with little wave or tidal action as there is little significant reworking of the turbidites.

CONCLUSIONS

Nineteen samples were taken from the Miocene section of CRP-1, between 90.25 - 146.50 mbsf. Using grain-size analysis, detailed core-logging, X-radiography, thin sectioning of microstructures, three main styles of gravity-flow sedimentation were established.

The dominant form of gravity-flow deposits are thin (centimetre-scale) muddy debris-flow deposits. These are characterised by very poorly sorted, faintly laminated muddy sandstones with coarse granules toward the base. Contacts are gradational to sharp. Occasionally these become rhythmically stacked sequences of pebbly-coarse sandstones indicating successive thin debris-flow events. These suggest very high sedimentation rates on an unstable slope in a shallow-water proximal glacimarine environment. Sandy-silty turbidites are indicated by inversely to normally graded well-laminated siltstones with occasional lonestones. These events are more characteristic of a distal shallow-water glacimarine environment and appear more common in the lower sections of the core, below approximately 141.00 mbsf, although occasionally occurring with the debris flows.

ACKNOWLEDGEMENTS

Many thanks to all the people at Scott Base, Ross Island who made us all so welcome during our stay. Thanks also to Mike Tabecki for the difficult thin-section work both here at British Antarctic Survey and at McMurdo Station. Laura De Santis and Ross Powell are thanked for help with the difficult X-radiography of the core at the Crary Laboratory, McMurdo Station. The paper was greatly improved by the critical reviews of Carol Pudsey, Mike Thomson, Ross Powell, Peter Barrett and Mike Hambrey.

REFERENCES

- Akhurst M.C., 1991. Aspects of Late Quaternary sedimentation in the Faeroe-Shetland Channel, North-West UK Continental Margin. *British Geological Survey, Technical Report*, WB/91/2.
- Barrett P.J., 1996. Antarctic Palaeoenvironment through Cenozoic Times. *Terra Antarctica*, **3**(2), 103-119.
- Barrett P.J. & Hambrey M.J., 1992. Plio-Pleistocene sedimentation in Ferrar Fjord, Antarctica. *Sedimentology*, **39**, 109-123.
- Barrett P.J., Hambrey M.J., Harwood D.M., Pyne A.R. & Webb P.N., 1989. Synthesis of CIROS-1 drillhole. In: Barrett P.J. (ed.) *Antarctic Cenozoic history from the CIROS-1 drillhole, McMurdo Sound, DSIR Bulletin*, **245**, 241-251.
- Bartek L.R. & Anderson J.B., 1991. Facies distribution resulting from sedimentation under polar interglacial climatic conditions within a high-latitude marginal basin, McMurdo Sound, Antarctica. In: Anderson J.B. & Ashley G.M. (eds.) *Glacial marine sedimentation; Paleoclimatic significance*, Boulder, Colorado, *Geological Society of America, Special Paper*, **261**, 223-226.
- Cape Roberts Science Team, 1998. Summary of Results from CRP-1, Cape Roberts Project, Antarctica. *Terra Antarctica*, **5**(1), 125-137.
- Dowdeswell J.A., Kenyon N.H., Laberg J.S. & Elverhoi A., 1997. Submarine debris flows on glacier-influenced margins: GLORIA imagery of the Bear Island Fan. In: Davies T.A., Bell T., Cooper A.K., Josehams H., Polyak L., Solheim A., Stoker M.S. & Stravers J.A., *Glaciated Continental Margins: an Atlas of Acoustic Images*, Chapman & Hall, London.
- Eyles C.H., Eyles N. & Miall A.D., 1985. Models of glaciomarine sedimentation and their applications to the interpretation of ancient glacial sequences. *Palaeogeography, Palaeoclimatology, Palaeoecology*, **51**, 15-84.
- Fielding C.R., Woolfe K.J., Purdon R.G., Lavelle M. & Howe J.A., 1997. Sedimentological and Stratigraphical Re-Evaluation of the CIROS-1 core, McMurdo Sound, West Antarctica. *Terra Antarctica*, **4**(2), 149-160.
- Hein F.J., van Wagoner N.A. & Mudie P.J., 1990. Sedimentary facies and processes of deposition, Ice Island Cores, Axel Heiberg shelf, Canadian Polar Continental Margin. *Marine Geology*, **57**, 243-265.
- Hill P.R., 1984. Sedimentary facies of the Nova Scotian upper and middle continental slope, offshore eastern Canada. *Sedimentology*, **31**, 293-309.
- Howe J.A., 1995. Sedimentary processes and variations in slope-current activity during the last Glacial-Interglacial episode on the Hebrides Slope, northern Rockall Trough, North Atlantic Ocean. *Sedimentary Geology*, **96**, 201-230.
- Johnson R.J. & Semple R.K., 1983. Classification using information statistics. *Concepts and Techniques in Modern Geography*, **37**, 38 p.
- Pickering K., Hiscott R.N. & Hein F.J., 1989. *Deep-marine environments: clastic sedimentation and tectonics*. Unwin Hyman, London.
- Semple R.K., Youngman C.E. & Zeller R.E., 1972. Economic regionalization and information theory; An example. *Discussion Paper 28, Department of Geography, Ohio State Univ. Columbus*, 64 p.
- Stow D.A.V., 1979. Distinguishing between fine-grained turbidites and contourites on the Nova Scotian deep water margin. *Sedimentology*, **26**, 371-387.
- Woolfe K.J. & Michibayashi K., 1995. Basic Entropy grouping of laser-derived grain-size data - an example from the Great Barrier Reef. *Computers and Geosciences*, **21**(4), 447-462.
- Wright R. & Anderson J.B., 1982. The importance of sediment gravity-flow to sediment transport and sorting in a glacial-marine environment: Weddell Sea, Antarctica. *Geological Society of America Bulletin*, **93**, 951-963.